

# The mechanics of a climbing fall with a belayer who can be lifted

January 2021

Ulrich Leuthäusser

## Abstract

In sport climbing, a common method of belaying is to use a static rope brake attached to the belayer's harness, but the belayer can move freely.

This paper investigates the dynamics of a climbing fall with such a belayer. The dynamics are nontrivial because of the belayer's constraint to be always at or above his initial position. An exact solution for a linear elastic rope is presented.

Compared to a fix-point belay, one obtains a considerable force reduction on the belay-chain. However, there is a trade-off of a longer stopping distance of both climber and belayer.

In order to calculate the stopping distance, friction between rope and the top carabiner has been taken into account. Closed-form formulas allow for calculating the maximum impact force, as well as the minimum mass of the belayer which is necessary to hold a fall from a certain height.

## Acknowledgement

The author thanks Ira Leuthäusser for helpful discussions and critical reading of the manuscript.

## Introduction

A climbing fall exerts considerable forces on the belay chain, consisting of the climber, protection points, rope and belayer. Several belay techniques are available, depending on the attachment of the belay device and its dynamic behavior. The selected technique strongly influences the motion of the climber and belayer during the fall, as well as the resulting forces. Thus, knowing their size in relation to the applied belay technique is of great importance for climbing safety.

In the simplest physical model, the climbing rope is treated as a linear frictionless oscillator. With this model, the maximum restoring force of the rope, sometimes called impact force, and its maximum elongation can be simply calculated [1,2]. More complicated models take into account the viscoelastic behavior of the rope [3,4], as well as the non-linearity of its force-elongation curve [4]. In this context, the fast elongation of the rope has to be treated thermodynamically as an adiabatic process [4]. As a consequence, dissipation is small up to almost the maximum force. The frictionless linear oscillator model is therefore an acceptable approximation of the maximum force on the rope.

In the above models, a static fix-point belay is generally assumed, that is, the rope is attached to a fixed anchor. While this scenario corresponds to the laboratory conditions of the UIAA standard fall, this scenario is not consistent with the normal climbing practice. In sport climbing, the majority of belayers use a body belay with a device like the Grigri, Click-up, Mega Jul or similar device which is attached to the harness. These devices are auto-locking, i.e. they act statically without any rope slip through the brake. Even classical braking devices like the Munter hitch (HMS) or tube devices, which are in principle dynamic, have a rather high force threshold for a rope slip through the brake. Thus, they are considered almost static brakes.

A body belay with a static brake inevitably pulls up the belayer. The same more exotic situation arises in the event of a fall when both the belayer and climber climb simultaneously with a more or less taut rope.

In semi-popular publications [5], various suggestions and recommendations about the appropriate belay method are circulating without any theoretical background. Detailed measurements are still missing. Only Petzl, the manufacturer of the Grigri, published some reasonably accurate experiments with the Grigri [6].

The purpose of this paper is to provide the theoretical background with an exact solution of the dynamics of a climbing fall with a movable belayer. For this belay method, an impact force formula is derived, replacing the standard fix-point belay impact force and is also compared with the mentioned climbing fall experiments. Furthermore, the stopping distances of climber and belayer are calculated to determine the allowed fall factors without hitting the ground.

## The climbing fall with a movable belayer without friction

Consider the situation shown in Fig.1. After a free fall of distance  $h$ , a climber C of mass  $m_1$  has the velocity  $v_1(0) = \sqrt{2gh}$  at  $P_1$ . He is connected to a rope of length  $L$  with a spring constant  $k$ . The rope, which is deflected by the protection point  $P_2$ , begins to stretch at  $P_1$  and slides without friction over  $P_2$ . The climber has the coordinate  $x_1$ , which cannot exceed  $L - h$ .

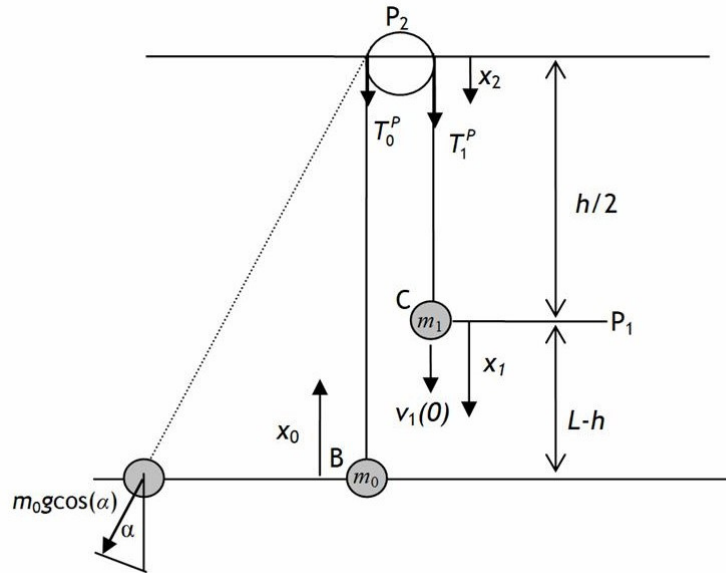


**Figure1** A belayer B of mass  $m_0$  is attached to a climber C of mass  $m_1$  who fell a distance  $h$  and has the velocity  $v_1(0)$  at  $P_1$ . The motion of B is described by the coordinate  $x_0$ , C by the coordinate  $x_1$ . At the protection point  $P_2$ , there are two tensions,  $T_0^P$  directed towards B and  $T_1^P$  directed towards C, which differ when friction is present. The displacement of the rope at  $P_2$  is  $x_2$ . If B has an angle  $\alpha$  to the vertical,  $m_0$  has to be replaced by the component  $m_0 \cos(\alpha)$  in the direction of the rope (dotted line).

If the belayer B is attached to a fix-point, that is  $x_0^{fp}(t) \equiv 0$ , the displacement  $x_1^{fp}$  of C is determined by the oscillator equation  $m_1 \ddot{x}_1^{fp} + kx_1^{fp} = m_1 g$ . Starting at  $t=0$  with the initial velocity  $v_1(0)$  from the taut rope position  $P_1$  and  $x_1^{fp}(0) = 0$ , it is given by Eq.(1):

$$x_1^{fp}(t, \omega, g) = \frac{v_1(0)}{\omega} \sin(\omega t) + \frac{g}{\omega^2} (1 - \cos(\omega t)) + x_1(0) \cos(\omega t), \quad (1)$$

with the frequency of oscillation  $\omega = \sqrt{k/m_1}$ . From Eq. (1), the well-known maximum impact force  $F_{\max}^{fp} = k \max(x_1^{fp}) = mg + \sqrt{(gm)^2 + 2gmkh}$  can be derived.

When B is not attached to a fix-point and can freely move vertically without being constrained by an impenetrable floor, the equations of motion for B and C are given by Eqs. (2a) and (2b):

$$m_0 \ddot{x}_0 + k(x_0 - x_1) = -m_0 g, \quad (2a)$$

$$m_1 \ddot{x}_1 + k(x_1 - x_0) = m_1 g. \quad (2b)$$

With relative and (shifted) center-of-mass coordinates

$$d = x_1 - x_0 \quad \text{and} \quad s = \frac{m_0 x_0 + m_1 x_1}{m_0 + m_1},$$

Eqs. (2a) and (2b) can be transformed into two decoupled equations for  $d$  and  $s$

$$\ddot{d} + \Omega^2 d = 2g, \quad (3a)$$

$$\ddot{s} = \frac{m_1 - m_0}{m_1 + m_0} g, \quad (3b)$$

with the frequency  $\Omega = \sqrt{k/m_r}$  and the reduced mass  $m_r = \frac{m_0 m_1}{m_1 + m_0}$ .  $m_r$  is half the harmonic mean of the masses  $m_1$  and  $m_0$ . The center-of-mass motion  $s$  of Eq. (3b) represents the motion of the famous Atwood fall machine.

In Eq. (3a), the coordinate  $d$  describes the same harmonic motion as the fix-point  $x_1^{fp}$  only with a different frequency and a different external force. Therefore, the unconstrained  $d^u(t)$  can be obtained from  $x_1^{fp}(t, \omega, g)$  of Eq. (1) simply by replacing  $\omega$  by  $\Omega$  and  $g$  by  $2g$ , that is

$$d^u(t) \equiv x_1^{fp}(t, \Omega, 2g).$$

The initial conditions are  $d^u(0) = x_1^u(0)$  and  $\dot{d}^u(0) = v_1(0)$  assuming that  $x_0$  starts from a rest position  $\dot{x}_1^u(0)$ . The superscript  $u$  denotes the unconstrained motion. Together with the solution of Eq. (3b), the result is shown in Eq. (4):

$$s^u(t) = \frac{1}{2} g \frac{m_1 - m_0}{m_1 + m_0} t^2 + \frac{m_1}{m_1 + m_0} (x_1^u(0) + v_1(0)t), \quad (4)$$

and Eqs. (2a) and (2b) are solved by Eqs. (5a) and (5b):

$$x_0^u(t) = s^u(t) - \frac{m_1}{m_1 + m_0} d^u(t), \quad (5a)$$

$$x_1^u(t) = s^u(t) + \frac{m_0}{m_1 + m_0} d^u(t).$$

(5b)

The maximum restoring force is shown in Eq. (6a):

$$F_{\max}^u = k d_{\max}^u = k \max(x_1^{fp}(t, \Omega, 2g)) = m_r \left( 2g + \sqrt{(2g)^2 + v_1(0)^2 \Omega^2} \right). \quad (6a)$$

Written in terms of the fall factor  $f=h/L$ , cross section  $Q$  of the rope and effective modulus of elasticity  $E = kL/Q$ , Eq. (6a) can also be written as shown in Eq. (6b)

$$F_{\max}^u = 2m_r g + \sqrt{(2gm_r)^2 + 2gm_r E Q f}. \quad (6b)$$

Now the non-holonomic constraint

$$x_0(t) \geq 0 \quad (7)$$

is introduced to take into account that B can never be below the ground.

The expansion of  $x_0^u(t)$  for short times  $x_0^u(t) \approx -1/2 g t^2 + O(t^3)$  shows that  $x_0^u(t)$  always starts with a downward motion violating the constraint. Thus, Eqs. (5a) and (5b) are not solutions of the constrained problem.

Based on Eq. (2b), when the restoring force of the rope  $kx_1$  becomes larger than  $m_0 g$ , B gets an upward net force and is lifted. This happens at the take-off time  $t_0$  given by Eq. (8):

$$kx_1^{fp}(t_0) = m_0 g. \quad (8)$$

For  $t < t_0$ , the constrained  $x_0(t)$  is zero and the fix-point solution is valid.  $t_0$  is given by Eq. (9):

$$t_0 = \frac{2}{\omega} \arctan \left[ \frac{\sqrt{(v_1(0)\omega \cdot m_1/m_0)^2 + g^2(2m_1/m_0 - 1) - v_1(0)\omega\rho}}{g(2m_1/m_0 - 1)} \right], \quad (9)$$

as long as the square root is real, that is  $m_0 < m_1 + m_1\sqrt{1 + v_1(0)^2 \omega^2 / g^2}$ .

For a larger  $m_0$  there is no take-off at all. The expansion of Eq. (9) for small times gives the excellent approximation  $t_0 \approx m_0 g / kv_1(0)$ .

When B takes off at  $t_0$ , Inequality (7) is fulfilled and therefore Eqs. (5a) and (5b) are valid until B comes back to the ground, assuming that C does not reach the ground first. This happens at time

$$t_1 \approx 2m_1 v_1(t_0) / g(m_0 - m_1) \text{ for } m_0 > m_1.$$

In this paper,  $t_1$  is considered as an end point because the further motion of B after touching the ground depends on how the collision with the ground is treated, which is not of interest here.

With the previous  $x_1^{fp}$  and  $x_0^u$ , it is possible to determine the exact piecewise solution with the constraint (7) as shown in Eqs. (10a) and (10b):

$$x_0(t) = \begin{cases} 0 & t \leq t_0 \\ x_0^u(t - t_0) & t_0 < t < t_1 \end{cases}, \quad (10a)$$

$$x_1(t) = \begin{cases} x_1^{fp}(t) & t \leq t_0 \\ x_1^u(t - t_0) & t_0 < t < t_1 \end{cases} \quad (10b)$$

The initial conditions of B are  $x_0(0) = 0$  and  $v_0(0) = 0$ .  $x_1^u(t_0) = x_1^{fp}(t_0)$  and  $v_1^u(t_0) = v_1^{fp}(t_0)$  have to be used at time  $t_0$ .  $\dot{x}_{0,1}(t)$  and  $\ddot{x}_{0,1}(t)$  can be simply obtained by differentiating  $x_1^{fp}(t)$  and  $x_0^u(t - t_0)$  in Eqs. (10a) and (10b) once or twice.

Figure 2 shows the exact displacements  $x_0(t)$  and  $x_1(t)$  of B and C and the forces  $m_0a_0(t)$  and  $m_1a_1(t)$  calculated with Eqs. (10a) and (10b). The parameters describe a typical climber fall in the initial phase of a climb:  $h=3$  m,  $L=6$  m, and  $m_0=50$  kg and  $m_1=70$  kg. The motion of B starts at the take-off time  $t_0$  and is delayed compared to C. At the time where F has its maximum,  $x_0(t)$  is still small, while  $x_1(t)$  has almost reached a plateau. The forces acting on B and C are approximately the same.

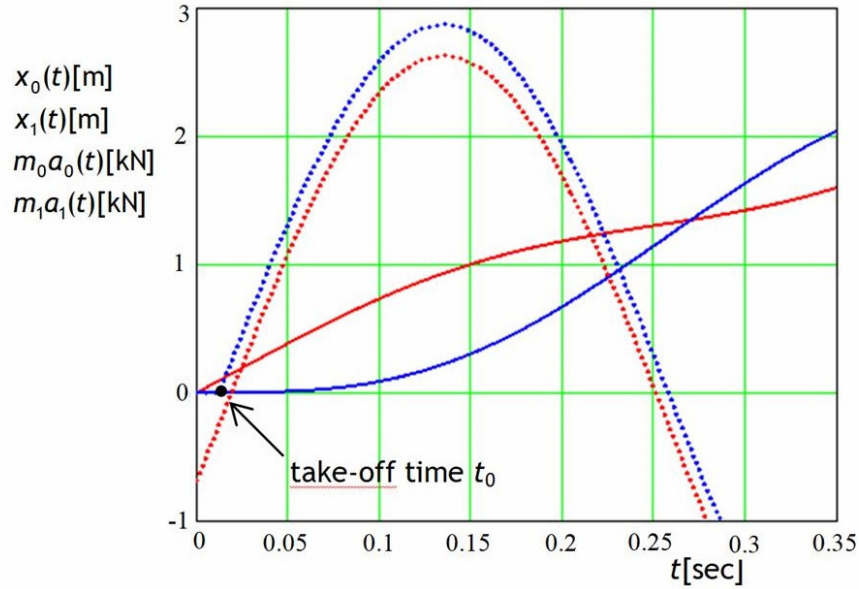


**Figure 2** Plot of the displacement  $x_0(t)$  of the belayer B (solid blue) and the force  $m_0a_0(t)$  (dotted blue), which acts on him and correspondingly  $x_1(t)$  (solid red) and  $m_1a_1(t)$  (dotted red) for the climber C.

The maximum restoring force of the rope  $F_{\max} = k \max[d^u(t - t_0)]$  can now be calculated with the result shown in Eq. (11):

$$F_{\max} = \begin{cases} F_{\max}^{fp} = m_1g + m_1\sqrt{g^2 + v_1(0)^2 \omega^2} & m_0 \geq m_1 + m_1\sqrt{1 + v_1(0)^2 \omega^2 / g^2} \\ 2m_rg + m_r\sqrt{(2g - x_1^f(t_0)\Omega^2)^2 + v_1^f(t_0)^2 \Omega^2} & m_0 < m_1 + m_1\sqrt{1 + v_1(0)^2 \omega^2 / g^2} \end{cases}, \quad (11)$$

The unconstrained maximum force  $F_{\max}^u$  of Eq. (6b) becomes a good approximation for  $F_{\max}$  when  $m_1/m_0 > 2g/\omega v_1(0)$ .

In Fig. 3, the exact  $F_{\max}$  of Eq. (11) is shown together with its approximation  $F_{\max}^u$  as a function of  $m_1/m_0$ . For  $m_1/m_0 = 2g/\omega v_1(0)$   $F_{\max}^u$  intersects  $F_{\max}^{fp}$ .

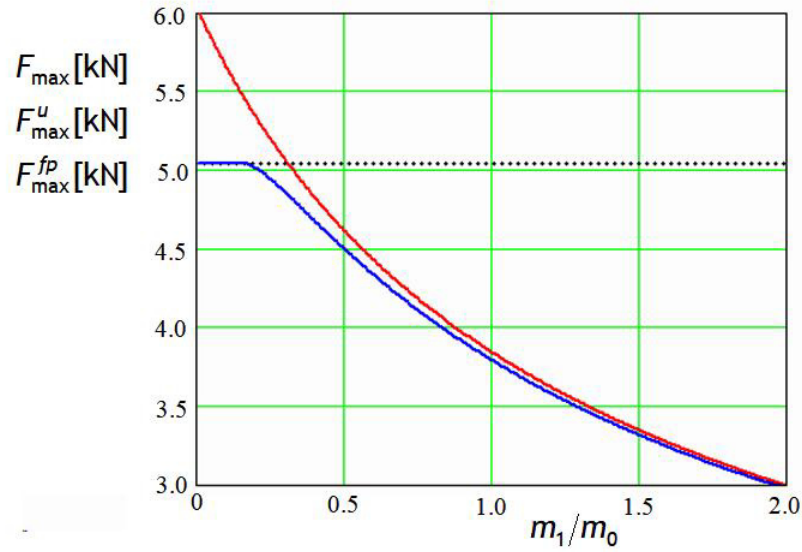


**Figure 3** The exact  $F_{max}$  (solid blue) from Eq. (11), its approximation  $F_{max}^u$  (solid red) from Eq. (6) in kN for  $v_0=7.67\text{m/sec}$ ,  $f=0.5$ ,  $L=6\text{ m}$  and  $h=3\text{ m}$ . The used spring constant  $k=3.7\text{ kN/m}$  is typical for a single rope. The horizontal dotted line is the fix-point  $F_{max}^{fp}$  and coincides with  $F_{max}$  in the limit  $m_0 \rightarrow \infty$ . The maximum relative error  $F_{max}^u / F_{max} - 1$  is smaller than 2.6% in the range of  $0.5 < m_1/m_0 < 1.5$ .

Comparing  $F_{max}$  with the fix-point  $F_{max}^{fp}$ , one obtains for larger falls ( $\omega \cdot v_1(0) \gg g$ )

$$\frac{F_{max}}{F_{max}^{fp}} \approx \frac{m_r \Omega}{m_1 \omega} = \frac{1}{\sqrt{1 + m_1/m_0}}. \quad (12)$$

Thus, a movable belaying mass with the same mass as the climber typically leads to a smaller impact force of approximately 30%. This is a surprisingly large reduction, which also exists for the forces on B and C as well as on the force  $2F_{max}$  on the protection point  $P_2$ . Remarkably, the force ratio in Eq. (12) is independent of the spring constant  $k$  or the material constant  $E$ .

The maximum forces on B and C are given by  $F_{Bmax} = F_{max} - m_0g$  and  $F_{Cmax} = F_{max} - m_1g$ .

If B jumps off the ground with velocity  $v_0(0)$ , the difference  $v_1(0) - v_0(0)$  enters the maximum  $F$  of Eq. (6b), which is then changed to Eq. (13):

$$F_{max} \approx 2m_r g + m_r \sqrt{(2g)^2 + (v_1(0) - v_0(0))^2 \Omega^2}. \quad (13)$$

Assuming that the movable belayer hits the start time exactly, he can reduce  $F_{max}$  by an additional factor  $(1 - v_0(0)/v_1(0))$ . Also, the opposite sign of  $v_0(0)$  is possible: dangerously large forces can appear when the belayer moves quickly backwards during the climber's fall.

$F_{max}$  occurs at time

$$T = \frac{1}{\Omega} \left( \arctan \left( \frac{2g}{v_1(0)\Omega} \right) + \frac{\pi}{2} \right) \cong \frac{\pi}{2\Omega} + 2 \frac{g}{\Omega^2 v_1(0)} .$$

The lengthy exact displacements  $x_0(T)$  and  $x_1(T)$  can be replaced by the approximate expressions good enough for larger falls ( $g/\Omega v_1(0) \ll 1$ ) as shown in Eqs. (14a) and (14b):

$$x_1(T) \cong \frac{v_1(0)}{\Omega} \frac{\pi/2 \cdot m_1 + m_0}{m_1 + m_0} , \quad (14a)$$

$$x_0(T) \cong \left( \frac{\pi}{2} - 1 \right) \frac{v_1(0)}{\Omega} \frac{m_1}{m_1 + m_0} . \quad (14b)$$

For values  $m_1/m_0$ , in practice between 0.5 and 1.5,  $x_1(T)$  is close to the fix-point  $\max(x_1^{fp}) \cong v_1(0)/\omega$  .

From Eqs. (4) and (5), for  $m_0 < m_1$ , the velocity of C always stays positive until C hits the ground. When  $m_0 > m_1$ , C changes the sign of his initial velocity and  $s(t)$  reaches its maximum

$$s_{\max} = \frac{v_1(0)^2}{2g} \frac{m_1^2}{m_0^2 - m_1^2} . \quad (15)$$

## The climbing fall with a movable belayer with friction

Under real conditions, there is no divergence of  $s_{max}$  of Eq. (15) for  $m_0 \rightarrow m_1$ . After a fall, B and C of equal weight will stop and C will not hit the ground with half his initial velocity  $v_1(0)/2$ . Thus, to get a realistic description, one has to include sliding friction between the rope and the top carabiner.

This is done by introducing the auxiliary displacement variable  $x_2$  at the deflection point  $P_2$ . Eqs. (2a) and (2b) take the form:

$$m_1 \ddot{x}_1 = m_1 g - k_1(x_1 - x_2), \quad (16a)$$

$$m_0 \ddot{x}_0 = -m_0 g + k_0(x_2 - x_0). \quad (16b)$$

The spring constants  $k_0$  between  $x_0$  and  $x_2$  and  $k_1$  between  $x_1$  and  $x_2$  are given by

$$k_0 = \frac{L}{L-h/2} k \quad \text{and} \quad k_1 = \frac{L}{h/2} k.$$

The elastic forces in Eqs. (16a) and (16b) act on B and C. The tensions  $T_{0,1}^P$  at the deflection point  $P_2$  have opposite signs as these forces as shown in Eq. (17)

$$\begin{aligned} T_1^P &= k_1(x_1 - x_2) > 0, \\ T_0^P &= -k_0(x_2 - x_0) < 0. \end{aligned} \quad (17)$$

The Euler-Eytelwein equation relates these two tensions

$$-T_0^P = T_1^P \kappa, \quad (18)$$

with  $\kappa = e^{-\beta\mu}$ .  $\mu$  is the dynamic friction coefficient and  $\beta$  the angle of contact between the rope and top carabiner. When the belayer is directly below  $P_2$  (see Fig.1), one has  $\beta = \pi$ .

For several protection points,  $\beta$  is the sum of all turnarounds of the rope.

While the Euler-Eytelwein relation is usually applied to static friction, it is used here for sliding friction. Measured friction coefficients, which strongly depend on the surface coating and age of the rope, vary between 0.1 and 0.2. Equation (18) is valid as long as  $\dot{x}_2(t) > 0$ . In this case, the friction force  $R = |T_0^P| - T_1^P$  points in the negative x-direction.

Inserting the tensions from Eq. (17) into Eq. (18), one gets  $x_2 = (\kappa k_1 x_1 + k_0 x_0) / (k_0 + \kappa k_1)$  so that  $x_2$  can be eliminated from Eqs. (16). This leads to the equation of motion for  $d$  with friction as shown in Eq. (19):

$$\ddot{d} + \Omega_k^2 d = 2g, \quad (19)$$

with the changed frequency of oscillation

$$\Omega_k = \sqrt{\frac{k_0 k_1}{k_0 + \kappa k_1} \frac{m_0 + \kappa m_1}{m_0 m_1}}. \quad (20)$$

$k_\kappa = \frac{k_0 k_1}{k_0 + \kappa k_1}$  is an effective spring constant. The presence of friction increases the stiffness of the spring.

With  $d_{\max} = \frac{2g}{\Omega_\kappa^2} + \frac{1}{\Omega_\kappa^2} \sqrt{v_0^2 \Omega_\kappa^2 + 4g^2}$ , obtained from Eq. (19), the maximum restoring force is given in Eq. (21):

$$F_{\max}^\kappa = k_\kappa d_{\max} = \frac{m_1 m_0}{m_0 + m_1 \kappa} \left( 2g + \sqrt{v_0^2 \Omega_\kappa^2 + 4g^2} \right). \quad (21)$$

In contrast to the case without friction, the maximum forces on B and C are no longer the same because friction reduces the tension  $T_0^P$  (Eq. (18)). These forces are given by Eqs. (22a) and (22b):

$$F_{B\max}^\kappa = \max(|m_0 \ddot{x}_0|) = \kappa F_{\max}^\kappa - m_0 g, \quad (22a)$$

$$F_{C\max}^\kappa = \max(|m_1 \ddot{x}_1|) = F_{\max}^\kappa - m_1 g. \quad (22b)$$

In the fix-point case,  $\omega$  is also changed to  $\omega_\kappa = \sqrt{k_\kappa/m_1}$ , which must be taken into account for the comparison of  $F_{\max}^\kappa$  with the corresponding maximum fix-point force  $F_{\max}^{fp}$ .

For the ratio of the maximum forces for larger falls, one gets Eq. (23):

$$\frac{F_{\max}^\kappa}{F_{\max}^{fp}} \approx \sqrt{\frac{1}{1 + \kappa m_1/m_0}}. \quad (23)$$

Friction reduces the effect on the moveable belyer and disappears completely in the case of large friction  $\kappa \rightarrow 0$ .

For the center-of-mass coordinate, one obtains Eq. (24):

$$\ddot{s} = -\frac{m_0 - \kappa m_1}{m_0 + \kappa m_1} g + \frac{1 - \kappa}{m_0 + \kappa m_1} \frac{m_1 m_0}{m_1 + m_0} \ddot{d}. \quad (24)$$

The second term on the right side of Eq. (19) for  $t_0 < t < 2T$  is always less than zero and therefore slows down the motion of  $s$ . For a static rope with the constraint  $d \equiv 0$ , this term is zero. The travel distance of the center-of-mass coordinate of a static rope always exceeds the one of a stretchable rope.

When equation Eq. (24) is integrated, the integral  $\int_0^t \ddot{d}(t) dt = v_d(t) - v_d(0)$  appears with an unknown  $v_d(t)$ . The time scale on which  $v_d(t)$  goes to zero is of the order  $\pi/\Omega$  [sec]  $\sim 0.01\sqrt{2L}$  [m]. It is much shorter than the stopping time of  $s$ , which is of the order  $\sqrt{g/h}$ . Therefore,  $d$  is a fast relaxing variable and  $v_d(t)$  is already zero at the stopping time

of  $s$ , so one can write  $\int_0^t \ddot{d}(t) dt \cong -v_d(0) = -v_1(0)$ . With this simplification, the integrated

Eq. (24) becomes

$$v_s(t) = -\frac{m_0 - \kappa m_1}{m_0 + \kappa m_1} g t + v_1(0) \frac{\kappa m_1}{m_0 + \kappa m_1}. \quad (25)$$

The stopping condition is now

$$m_0 > \kappa m_1,$$

which is a weaker requirement for  $m_0$  than for the case without friction.

The maximum  $s$  from Eq. (15) changes to Eq. (26):

$$s_{\max} = h \frac{\kappa^2 m_1^2}{m_0^2 - \kappa^2 m_1^2}, \quad (26)$$

where  $h = v_1(0)^2 / 2g$  has been inserted. In contrast to the fix-point maximum elongation, which is proportional to  $\sqrt{f}$ , the relative distance  $s_{\max}/L$  is directly proportional to  $f$ . Because of the fast variable  $d$ , it contains no rope properties.

To prevent a fall on the ground, the final displacement  $x_{1\max}$  of C has to meet the condition

$$x_{1\max} < L - h,$$

which consists of the sum of  $s_{\max}$  and half of the small final static rope stretch  $d_\infty$  (see Fig. 1). Without friction, that rope stretch is simply given by  $d_\infty = L\varepsilon_\infty$ . The static elongation  $\varepsilon_\infty$  is 6-8% for all climbing ropes for the mass 80 kg. Using  $d_\infty$  as an approximation and adding  $d_\infty/2$  to  $s_{\max}$  from Eq. (26), one obtains Eq. (27) in terms of the fall factor  $f=h/L$

$$f < \left(1 - \frac{\varepsilon_\infty}{2}\right) \left(1 - \kappa^2 \frac{m_1^2}{m_0^2}\right). \quad (27)$$

In Fig. 4, the regions of allowed  $f$  for  $\kappa=0.6$  and  $\kappa=0.7$  are shown as functions of  $m_0/m_1$ . For decreasing belayer masses the range of safe fall factors rapidly goes to zero and for  $m_0/m_1 < \kappa$ , a fall can no longer be held by B.

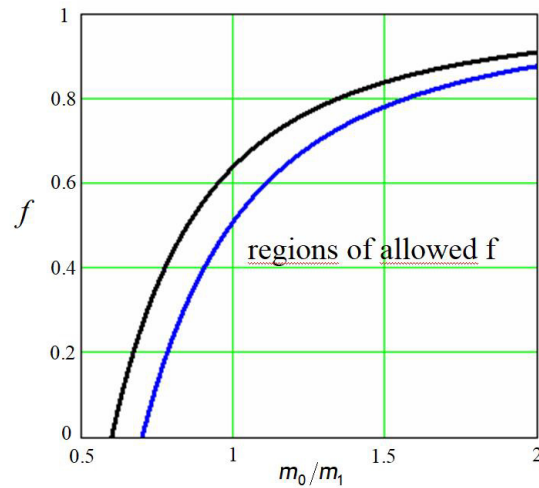


**Figure 4** Plot of the curves (Eq. 27) which separate the safe fall factors  $f$  from the prohibited  $f$  (with a fall hitting the ground) as functions of  $m_0/m_1$  ( $\kappa=0.6$  in black and  $\kappa=0.7$  in blue). The curves intersect the abscissa at  $\kappa$ . A higher friction coefficient increases the region of allowed  $f$ .

In general, the position of B is not directly below the first protection point. When B has an angle  $\alpha$  to the vertical (see Fig. 1), only the component of  $g$  in the direction of the rope acts against the tension  $T_0^P$  from the rope. Therefore the right hand side of Eq. (3a) has to be replaced by  $g(1 + \cos(\alpha))$ .

An additional equation of motion for  $\alpha$  describes the swing of B. This oscillatory motion is determined by the frequency  $\sqrt{g/L}$  which is much lower than  $\Omega$ , describing the longitudinal oscillation of the rope. Thus,  $\alpha$  remains almost unchanged until the force maximum. The corresponding formula to Eq. (6b) is

$$F_{\max}^u = m_r g(1 + \cos(\alpha)) + \sqrt{(g(1 + \cos(\alpha))m_r)^2 + 2gm_r EQf} .$$

The expansion  $F_{\max}^u \approx F_{\max}^u(\alpha = 0) - \frac{1}{2}m_r g\alpha^2$  for small  $\alpha$  shows that the correction to

$F_{\max}^u(\alpha = 0)$  is small.

## Fall experiments and their discussion

The theoretically determined impact forces from the last section are now compared with real impact forces [6]. These experiments consist of three series of test falls for three different rope lengths and fall heights. The masses of climber C and belayer B are both 80 kg. The test falls, in particular the first one, are representative of climbing falls with small fall factors, which often occur in sport climbing. This is in contrast to the heavy UIAA standard fall, which happens very rarely. While in the UIAA setup the main focus lies on the properties of the climbing rope, whereas the experiments by Petzl focus on the climber and his belayer.

In these test falls, the force on C differs considerably from the force on B, showing that dry friction between the rope and the protection points plays an important role for typical climbing falls. For the UIAA standard fall, however, dry friction can be neglected. The reason is due to the large fall factor near 2 with a very large  $k_0 \gg k_1$ , so that  $k_\kappa \approx k_1 \approx k$ . The results of the Petzl experiments are listed in Table 1. However, it would be desirable to have more detailed and accurate measurements, including stopping distances of B and C.

	fall test 1	fall test 2	fall test 3
1 rope length $L$ [m]	6.9	3	3.6
2 fall height $h$ [m]	2	2	3.6
3 fall factor $f=h/L$	0.29	0.67	1
4 $m_0, m_1$ [kg]	80, 80	80, 80	80, 80
5 angle $\alpha$ between B and first protection point	$\sim 18^\circ$	$\sim 27^\circ$	$\sim 34^\circ$
6 $\kappa$	0.7	0.7	0.55
7 $E \cdot Q$ [kN]	12.7	12.7	12.7
8 measured max. force [kN] on climber C	$\sim 2.5$	$\sim 3$	$\sim 4$
9 measured max. force [kN] on belayer B	$\sim 1.5$	$\sim 2$	$\sim 2$
10 calculated max. force on climber $F_{C_{\max}}^\kappa$ [kN] (Eq. 22b)	2.4	3.19	4.21
11 calculated max. force on belayer $F_{B_{\max}}^\kappa$ [kN] (Eq. 22a)	1.49	2.13	2.09
12 calculated max. impact force $F_{\max}^\kappa$ [kN] (max. tension)	3.19	3.97	4.99
13 calculated max. force on climber $F_{C_{\max}}^{fp}$ [kN] (fix-point)	2.88	4.15	5.13
14 calculated $s_{\max}$ [m]	2.39	ground fall	ground fall
15 force reduction $F_{C_{\max}}^\kappa / F_{C_{\max}}^{fp} - 1$ (line10/line13-1)	16.4%	23.1%	18%

Table 1: Fall tests [6] for different  $L$  and  $h$ . Measured impact forces on climber and belayer (lines 8 and 9) in comparison to the theoretically obtained forces (lines 10 and 11).

The measured impact forces of line 8 and 9 of Table 1 have to be compared with  $F_{C_{\max}}^\kappa$  and  $F_{B_{\max}}^\kappa$  of line 10 and 11 calculated from Eqs. (22a) and (22b).

The first fall test has been performed under conditions which are similar to those which have been assumed in the presented theory, i.e. only friction on the top carabiner, a small angle  $\alpha$  between B and C and minimal rope slack. Good agreement between theory and experiment is obtained with an error of only a few percent. However, more detailed measurements would be desirable.

The Euler coefficient  $\kappa = e^{-\pi\mu}$  has the value 0.7 with a chosen  $\mu = 0.125$ . The modulus of elasticity  $E$  times the cross section of the rope  $Q$  is 12.7 kN for all experiments.

Due to the small rope elongations for this fall with  $f=0.29$ , non-linear elastic behavior [4] of the rope can be neglected. Also, its viscoelastic behavior responsible for internal

friction is not very important for the maximum forces, because heavy damping occurs mainly in the backward motion of the rope after reaching its maximum elongation [4]. For the second fall experiment, a lanyard was used. Because the maximum forces occurred before the belayer was stopped by the rather long lanyard, a comparison with the theory is still possible. Again, good agreement with the measured impacts has been achieved. For the third experiment, the assumed friction has to be somewhat higher. This is not surprising, because the belayer hits his short lanyard very early with a lot of friction involved.

All test falls with a movable B differ significantly from a fall held by a fix-point belay. In Table 1, the force reductions on C with the movable B compared to the fix-point belay are approximately 20%.

How important is energy absorption of the bodies of the belayer and climber in a clean fall without hitting the wall? A rough order of magnitude estimation is presented to answer this question. Taking into account only soft body tissue, one obtains a modulus of elasticity  $E_h$  of the human body of approximately  $8 \cdot 10^7 \text{ N/m}^2$  [7]. With this value, it is possible to

estimate a lower bound of the spring constant  $k_h > E_h \frac{Q_h}{L_h} \approx E_h \frac{m_h}{\rho_h L_h^2} \approx 2 \cdot 10^6 \text{ N/m}$ , where the

values  $m_h = 80\text{kg}$ ,  $\rho_h = 10^3 \text{ kg/m}^3$  and  $L_h = 1.8\text{m}$  of an average person have been used. A typical spring constant of a climbing rope  $k_{\text{rope}}$  ( $L \sim 3\text{m}$ ) is approximately  $10^4 \text{ N/m}$ , which is two orders of magnitude softer than  $k_h$ .

For impact loading and B, the rope and C in series, it is easy to calculate the ratio of the stored elastic energy in the rope  $U_{\text{rope}}$  and the stored elastic energy  $U_h$  in the bodies of B and C. The result, neglecting friction, is

$$\frac{U_h}{U_{\text{rope}}} \approx 2 \frac{k_{\text{rope}}}{k_h} \sim 10^{-2}.$$

Because the human body is much stiffer than the rope, the transmitted energy  $U_h$  to B and C is much smaller than the energy  $U_{\text{rope}}$  absorbed by the rope. When small damping of the bodies of B and C is included, numerical calculations show no significant change of the above estimation.

Regarding the stopping distances, in the first test there is no risk for the climber to hit the ground. This agrees with Fig. 4, where the fall factor  $f=0.29$  is inside the region of allowed fall factors for  $m_0/m_1 = 1$ . In the second test, however, a ground fall would have occurred if the experiment had not been carried out in a multi-pitch environment, although  $f=0.67$  is considerably smaller than one. In Fig. 4, a fall with  $f=0.67$  is outside the region of allowed fall factors.

## Conclusion

In this paper, a climbing fall with a belayer who can be lifted off the ground has been investigated. Such a fall differs significantly from a fall held by a fix-point belay. For a linear elastic rope, the exact solution has been obtained combining piecewise solutions of the unconstrained problem without the ground and the solution for a fixed belayer. The solution is characterised by a lift of the belayer at a delayed take-off time. The exact solution of that mechanical problem is complicated and lengthy. It was shown that for the calculation of the maximum impact force for mass ratios that occur in practice, it is sufficient to use the much easier solution Eq. (6) of an unconstrained belayer. When friction is included, the form of the force Eq. (6) remains invariant, if the angular frequency and the reduced mass are appropriately redefined. The result is Eq.

(21). Furthermore, friction leads to a maximum distance which the belayer is pulled up (equal to the stopping distance of the climber) given approximately by  $s_{max}$  (Eq. (26)) when the small static rope elongation is neglected. If the mass  $m_0$  of the belayer is smaller than the mass  $m_1$  of the climber multiplied by the Euler coefficient  $\kappa$ ,  $s_{max}$  diverges with the consequence of hitting the ground.

As a trade-off to the lifting distance  $s_{max}$ , the appearing forces are much smaller due to the small reduced mass  $m_r$  of the belayer and climber which is now responsible for the impact force instead of the mass of the climber alone. For equal masses of a belayer and climber, the impact force  $F_{max}^{\kappa}$  is reduced to the fix-point  $F_{max}^{fp}$  of approximately  $1/\sqrt{1+\kappa} \sim 23\%$  for  $\kappa = 0.7$ .

Overall, the presented theory of a linear elastic rope with dry friction between rope and the protection points is able to explain the forces on the climber and his movable belayer in real climbing falls.

## References

- [1] Wexler A (1950) The theory of belaying. American Alpine Journal 7: 379-405
- [2] Gere JM, Goodno BJ (2009) Mechanics of materials 7<sup>th</sup> edn. Cengage Learning, Toronto pp 153-157
- [3] Pavier M (1998) Experimental and theoretical simulations of climbing falls. Sport Eng 1: 79-91
- [4] Leuthäusser U (2017) The physics of a climbing rope under a heavy dynamic load. Proc IMechE, Part P: J Sports Engineering and Technology 231(2): 125-135
- [5] Hellberg F, Hummel C, Steinmüller S (2014) <https://docplayer.net/39111765-Belaying-in-multi-pitch-routes-comfortable-or-secure.html>
- [6] Petzl (September 2020) Forces at work in a real fall. <https://www.petzl.com/US/en/Sport/Forces-at-work-in-a-real-fall?ActivityName=rock-climbing>
- [7] Tan XG, Kannan R, Przekwas AJ (2012) A comparative study of the human body finite element method under blast loadings. Proceedings of the ASME 2012 International Mechanical Engineering Congress & Exposition